

Scramjet Experiments in an Expansion Tunnel: Evaluated Using a Quasi-Steady Analysis Technique

Matthew McGilvray,* Richard G. Morgan,† and Peter A. Jacobs‡
University of Queensland, St. Lucia, Queensland 4072, Australia

DOI: 10.2514/1.J050024

As scramjet engine development moves toward higher and higher speeds, it will be important to continue to ground test complete nose-to-tail configurations at true flight conditions. Above Mach 10, the freestream total pressure requirements can only be met by an expansion-tube facility. To establish the practicality of ground-testing complete scramjet configurations at high Mach numbers, an expansion-tunnel facility is used to test a generic two-dimensional scramjet at a Mach 10 replication condition. As the flow produced in an expansion-tube facility is transient in nature, a method for analyzing point measurements within the scramjet is developed. A transient numerical simulation of the engine configuration without fuel injection is used to verify the validity of the technique, as well as to provide a reference data set for comparison to experimental data. These experiments show that stable supersonic combustion is established during the test time. Using the developed transient analysis, accurate quasi-steady pressure data at true flight conditions can be inferred from scramjet test measurements in an expansion-tube facility.

Nomenclature

H	=	stagnation enthalpy, J/kg
L	=	length, m
M	=	Mach number
p_p	=	pitot pressure, Pa
p_s	=	static pressure, Pa
Re_u	=	unit Reynolds number, 1/m
T_s	=	static temperature, K
t_t	=	test time, s
U	=	axial velocity, m/s
U_{norm}	=	normalization velocity, m/s
V	=	transverse velocity, m/s
W	=	spanwise velocity, m/s
x	=	axial distance, m
x_n	=	normalization axial position, m
x_{ref}	=	reference axial position, m
y	=	transverse distance, m
z	=	spanwise distance, m
λ	=	any given flow property
ρ	=	density, kg/m ³
ϕ	=	fuel equivalence ratio

I. Introduction

MANY types of facilities around the world have been used to test scramjets, such as heated blowdown facilities, long-duration piston compression facilities, and reflected shock tunnels. However, with the high-total-pressure and total-enthalpy requirements at the higher-Mach-number portion of the predicted transatmospheric scramjet ascent trajectory [1] (above 120 MPa and 4 MJ/kg), these facilities are incapable of matching all flow properties above a flight Mach number of 10. This is because they operate by processing the

test air to its stagnation properties before allowing it to expand to the desired flow conditions. This causes severe erosion of the shock-tube reservoir and nozzle throat region. As a result, these flow conditions are limited in total pressure to about 120 MPa [2]. Another undesirable effect is that the flow produced will be in a state of chemical nonequilibrium. Because the gas is expanded from stagnation conditions, in which the air is highly dissociated due to high temperatures (~3000 K at Mach 12), the dropping temperature drives the dissociated atoms to reform into binary molecules. However, due to the short transit times, some of the atoms will not have the time to recombine and therefore will not reach equilibrium composition [2]. As indicated by Curran [3], the need for very-high-enthalpy ground-test facilities is a vital part for scramjet engine development. Therefore, there is a need for a suitable ground-test facility for the higher-speed end of the scramjet operating envelope.

An alternative facility that can be used is the expansion tube, which is capable of producing the high-energy and high-density flows required for the development of high-speed scramjets [4]. It avoids the issues of high-total-pressure containment and nonequilibrium gas composition seen in other hypersonic ground-test facilities, because the test gas is never stagnated once the energy has been added to it. Instead, part of the energy addition to the test gas occurs through the unsteady expansion process after the test gas is initially processed by a shock wave. Coupled with a high-performance driver, the expansion tube is capable of producing total pressure to the order of tens of gigapascals [2]. However, there is a penalty and the expansion-tube facility can only provide relatively short test times related to the facilities geometric size. Also, expansion tubes have shown a tendency to produce inherently *noisy* flow [5] in the operating region where scramjets are to be tested. Conditions that are at the lower-enthalpy end of the expansion tube's likely operating range (below approximately 10 MJ/kg) and have a sound speed ratio over the test-gas/driver-gas interface close to unity exhibit this corrupted flow. If these shortcomings can be overcome, an expansion tube can provide a crucial ground-testing capability for propulsion testing, which is necessary for scramjet technology development to higher Mach numbers.

The ability to test scramjets in expansion tubes has been previously investigated by ATK-GASL, Inc., operating the HYPULSE (hypersonic pulse) facility in SET (shock-expansion tube) mode. Preliminary work by Rizkalla et al. [4] indicated that test conditions could be produced between Mach 15 and 20 for scramjet combustor tests with test times of approximately 200 μ s at a constant enthalpy of 15 MJ/kg. These conditions were further extended to 20 MJ/kg, with total pressures of up to 400 MPa [6]. It was noted that there could be a limitation of low-enthalpy conditions due to transition, though could be avoided by increasing the Reynolds number. An increase in

Presented as Paper 2009-7414 at the 16th AIAA/DLR/DGLR International Space Planes and Hypersonic Systems and Technologies Conference, Bremen, Germany, 19-22 October 2009; received 24 June 2009; revision received 15 March 2010; accepted for publication 11 May 2010. Copyright © 2010 by the American Institute of Aeronautics and Astronautics, Inc. All rights reserved. Copies of this paper may be made for personal or internal use, on condition that the copier pay the \$10.00 per-copy fee to the Copyright Clearance Center, Inc., 222 Rosewood Drive, Danvers, MA 01923; include the code 0001-1452/10 and \$10.00 in correspondence with the CCC.

*Research Fellow, Centre for Hypersonics, Division of Mechanical Engineering. Member AIAA.

†Professor, Centre for Hypersonics, Division of Mechanical Engineering. Associate Fellow AIAA.

‡Senior Lecturer, Centre for Hypersonics, Division of Mechanical Engineering.

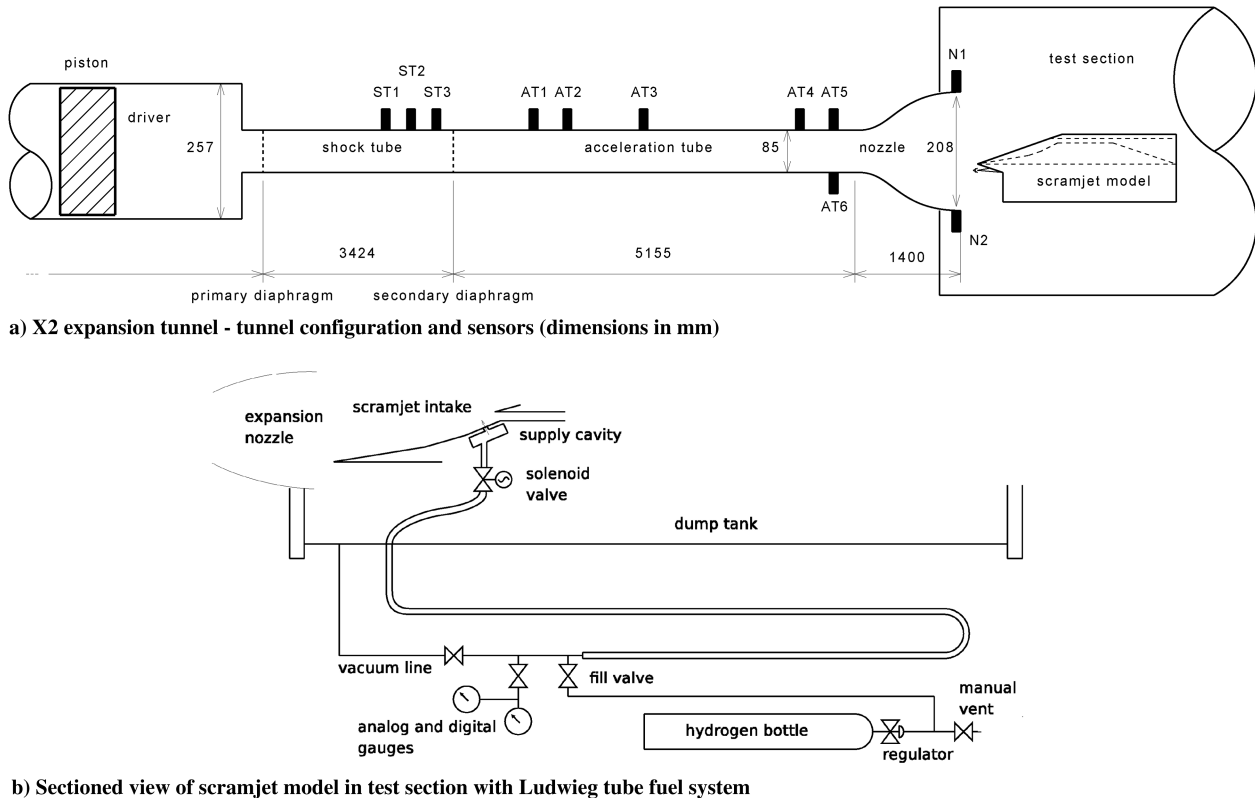


Fig. 1 Schematic of X2 expansion tunnel and arrangement of scramjet model in test section.

both static pressure capability and test time was shown to be possible with the inclusion of a detonation driver to the HYPULSE facility [7,8] running with a steady expansion nozzle. The design of a full capture nozzle by Chue et al. [9] led to the creation of a flight enthalpy condition. This was a Mach 15, 47.8 kPa dynamic pressure, flight-replication condition with a freestream Mach number of 13.5. This is a semidirect flow condition, requiring part of the intake to be removed to correctly ascertain the properties at the combustor entrance. A series of flight enthalpy conditions have now been produced between Mach 15–21 in the facility with test times of the order of 0.3 ms [10]. However, true flight conditions are yet to be created in any expansion tubes in the region of flight Mach numbers between 10–15, which is of more immediate, and possibly ultimate, interest.

This paper establishes the practicality of *nose-to-tail* scramjet testing in an expansion-tunnel facility at a flow condition that replicates true flight. This study targets the high-speed regime where reflected shock tunnels fail to produce flow with correct gas composition and vibrational state and fail to meet the high-total-pressure requirements. A flow condition is produced in expansion-tunnel mode (a steady expansion nozzle connected to the end of the acceleration tube) to avoid test time limitations caused by tube wall boundary-layer transition [11]. Specifically, a subscale scramjet

engine is tested at a Mach 10 flight-replication condition in the X2 expansion tunnel, which is at the current limitation of reflected shock tunnels. This extends from the HYPULSE work by testing a complete scramjet model at a flow condition with lower total enthalpy. This gives designers an important experimental tool; to test complete flow interaction with nominal freestream conditions at higher-Mach-number flight conditions. If used with other experimental techniques (such as direct combustor testing to account for long-duration heating effects) and numerical tools, scramjet performance can be seriously explored near the theoretical upper limit of scramjet operating range in terms of both total pressure and total enthalpy. The current paper shows that meaningful data can be produced in the short test times available in the expansion-tunnel facility.

II. Experimental Setup

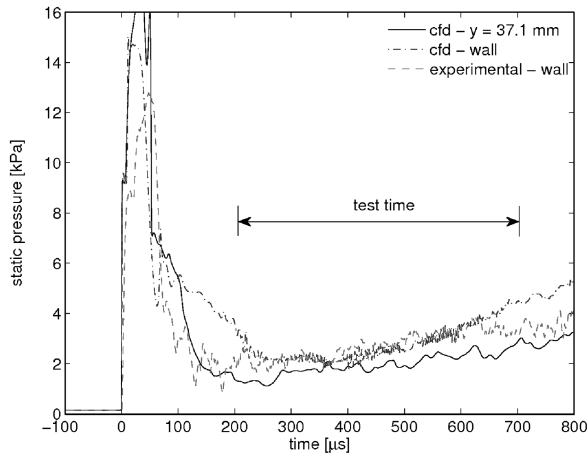
This experimental study was undertaken using the X2 free-piston expansion-tube facility [12] (Fig. 1a), located at the University of Queensland. A steady expansion nozzle was attached to the end of the acceleration tube for this experimental setup (this configuration is commonly known as an *expansion tunnel*). The inclusion of the nozzle has multiple effects on the flow production, such as increased test time and increased flow diameter. This comes at the expense of a lower total pressure and ρL simulation capability; however, this is not an issue for this experiment. In this scramjet experiment, the primary reason for the inclusion of the nozzle was to avoid the core flow diminishing effects caused by boundary-layer transition on the facility walls [11]. This has been a major restriction on scramjet test conditions that are suitable for simulation in expansion-tube facilities [5].

The scramjet was orientated in a body-side-down configuration for mounting to the test section rail (Fig. 1a). The scramjet is fueled with hydrogen from a plenum chamber behind the model, which requires constant stagnation properties during the test time. This is achieved by use of a Ludwig tube with a fast-response valve that can open in 10 ms, with the fuel mass flow rate interpreted via a pressure transducer mounted in the plenum chamber. A schematic of the fueling arrangement is shown in Fig. 1b. Fuel is required to be injected before the arrival of the startup flow, to maximize the test time after flow

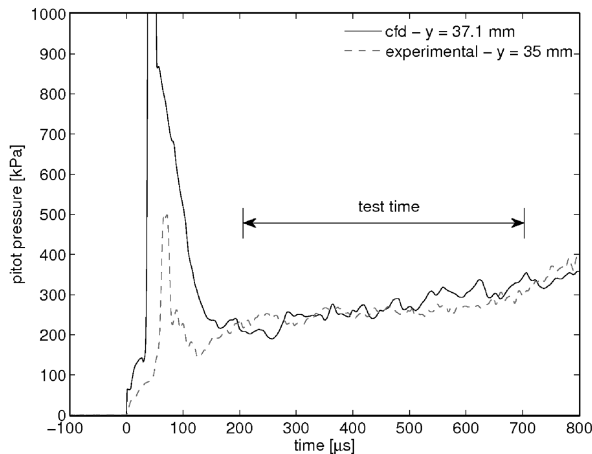
Table 1 Flow conditions for Mach 10 replication condition in the X2 expansion-tunnel facility

Property ^a	Experimental measurements	Calculations
p_s , kPa	2.4 ± 0.17	2.31 ± 0.30
p_p , kPa	292 ± 12	295 ± 46
M	—	10.1 ± 0.42
ρ , kg/m ³	—	0.029 ± 0.0037
T_s , K	—	245 ± 15
U , ms ⁻¹	—	3190 ± 100
H , MJ/kg	—	5.33 ± 0.39
Re_u , 10 ⁶ /m	—	5.89 ± 0.73
t_t , μ s	550 ± 20	560 ± 20

^aProperties are averaged over the test time, as defined in the text.



a) Static pressure at nozzle wall



b) Pitot pressure at 14 mm radially from centerline

Fig. 2 Comparison of numerical simulation and experimental data at nozzle exit for X2 Mach 10 condition.

establishment. However, if the fuel is injected too early, a substantial amount of hydrogen can propagate into the acceleration tube altering the flow condition produced. Triggering of the solenoid valve is needed before the primary diaphragm ruptures, since the time between diaphragm rupture and flow arrival is much less than valve opening time. The recoil movement of the facility from the free-piston compression is used to trigger the fuel valve. A more detailed description of the flow condition, design, and setup of the experiment can be found in McGilvray [11].

A. Flow Condition

The flow condition used in testing was scaled from a Mach 10 flight condition at a dynamic pressure 66 kPa. This flow condition created in the X2 facility required adjustment from the flight flow properties, as the core size/test time was smaller than that available in the parallel T4 experiments (discussed in the adjoining paper [13]). This prompted a two-fifths-scaled experiment (40×40 mm capture area) to be undertaken. Pulsonetti [14] explored scaling effects experimentally and concluded that the most appropriate scaling method for scramjet models is to maintain the ρL product. Therefore, the density in the X2 flow condition was increased by a factor of 2.5 over the flight condition. The flow properties averaged over the test time are given in Table 1, in which the test time is determined from pitot pressure measurements and reference to numerical predictions of the flow history.

Transient numerical simulations were conducted of the entire flow production using a hybrid modeling approach. This method simulates the driver and shock tube using a quasi-one-dimensional analysis, in which the transient history of properties at the secondary diaphragm are applied to the inflow boundary condition of a two-dimensional simulation of the acceleration tube. Further details of this calculation can be found in McGilvray [11]. Results of this calculation at the nozzle exit, averaged over the test time, are given in Table 1, in which numerical uncertainties are taken from Hayne [15]. A comparison of time histories of the experimental nozzle wall static pressure and pitot pressure (both at nozzle exit) and that from the numerical simulation of the facility is provided in Fig. 2. This reveals the transient nature of the flow, including both the unsteady starting process of the flow as well as transient behavior during the nominal test time.

For each shot, measurements are taken of the shock speeds and static pressures along the facility walls, as well as pitot pressure at nozzle exit. These measurements are used primarily to check if the flow production is within the bounds of experimental error, rather than account for shot-to-shot variation in scramjet data analysis. This is due to the large scale of the calculation (1092 CPU hours using 42 processors) required to compute flow conditions with any degree of accuracy.

B. Scramjet Design

It was desired to keep the scramjet design simple, as the focus of this experiment was to explore whether the expansion tube could be used to test a complete scramjet geometry. Therefore, the scramjet engine tested was a two-dimensional configuration (Fig. 3) with an axial length of 594.7 mm, using inlet (upstream) hydrogen injection [16]. The intake comprises an entropy-minimized four-shock intake, using three wedges. This was analytically optimized using shock relations, with viscous corrections applied after. The inlet captures a 40×40 mm area of flow and compresses it to the combustor height

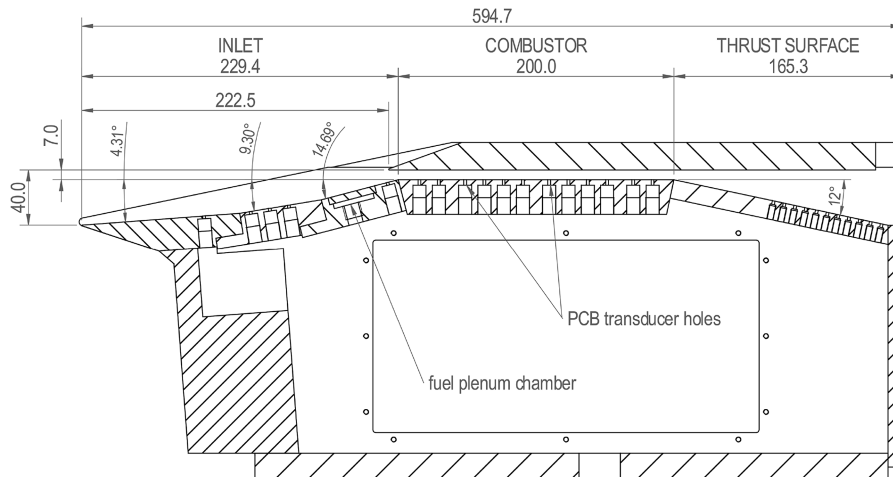


Fig. 3 Drawing of experimental Mach 10 scramjet model tested in X2. Sectioned down the midline of the engine. Dimensions are in millimeters.

of 7 mm, over an axial length of 292.7 mm (no sidewall compression). The combustor is 200 mm long and exhausts to a 12° thrust surface, taking the flow to the same area as the intake. Injection of the hydrogen was from a location 20 mm along the third wedge of the intake and at 45° to the local flow. The injectors were four evenly spread, 2-mm-diam holes, drilled through to the plenum chamber. Sidewall leading edges ran parallel to the bow shock along the intake and continued all the way through to the thrust surface exit. A larger-scale version of this engine has also been tested in the T4 reflected shock tunnel [13].

C. Sensors

Static pressure measurement gauges (PCB Piezotronics, Inc., model 112) were located along the body-side surface of the scramjet. Most measurements taken were on the centerline of the engine, apart from in the combustor in which several spanned the duct at several axial locations. Two measurements were taken on the thrust surface and were located 15 mm from the centerline. For all pressure measurements presented, the PCB pressure transducers were recess mounted. Additional measurements of fuel plenum pressure and Ludwig initial fill pressure were recorded in order to calculate the mass flow rate of hydrogen for each shot [11].

III. Analysis Technique for Quasi-Steady Flow

Where the flow into the scramjet is strongly transient, analysis of results must be undertaken that takes proper account of the unsteady nature. Point measurements of static pressure and heat transfer will be dependent on the time derivative change at that particular location. In contrast, integrated properties such as axial momentum, which dictate the total thrust of an engine, will be affected by the time derivative change in the property integrated within the control volume of the engine. The appropriate analysis is investigated for the correct description of static pressure measurements throughout the engine.

When considering the effects of unsteadiness on the flow through a scramjet for point measurements, it is useful to consider the *total derivative* of the flow properties from the Lagrangian point of view of a particle convecting through the flowfield [given in Eq. (1)] [17]. The total derivative of a given property λ ,

$$\frac{D\lambda}{Dt} = \frac{\partial\lambda}{\partial t} + U\frac{\partial\lambda}{\partial x} + V\frac{\partial\lambda}{\partial y} + W\frac{\partial\lambda}{\partial z} \quad (1)$$

contains both a local term $\partial\lambda/\partial t$ (which represents the transient nature of the flow property at a given point in space) and the convective terms $U(\partial\lambda/\partial x)$, $V(\partial\lambda/\partial y)$, and $W(\partial\lambda/\partial z)$ (which indicate how the flow property changes with time as a fluid particle moves to locations with different flow properties). If the local term is zero, the flow is therefore steady.

If the local term is nonzero, but much smaller than the convective terms, then particles will propagate through the flowfield in much the same way as they would in steady flow. Because of the coupling of any changes of velocity with changes in thermodynamic properties through the momentum and energy equations, the gas particle traversing the flowfield will have almost the same properties (i.e., pressure, temperature, density) as if the local term was zero. Such flows are called *quasi-steady* and the local flow properties can be used at any point in time to calculate the flowfield using a steady flow analysis.

For flows with high Mach numbers, the *hypersonic equivalence principle* [18] postulates that significant changes in Mach number may occur with only a small change in velocity, allowing for the flowfield to be described as unsteady flow in one less space dimension. In the case of a scramjet, if a planar slice of gas normal to the vehicles velocity is analyzed passing through the engine, different areas of the section will be processed differently as they pass down the duct due to waves altering the transverse/spanwise components of velocity. However, the bulk of the particles within a slice will all have similar axial velocities and will stay approximately adjacent to each other. Using the hypersonic equivalence principle, the flow through

the engine of a slice of gas normal to the vehicles velocity can be approximated to a single velocity component. Also, as the flow only undergoes small deflections in its velocity vector, the original axial speed (which is normal to the intake plane) can also be used to follow the slice of gas. Thus, the convective terms in the *total derivative* [Eq. (1)] can be based purely on the axial direction term $U(\partial\lambda/\partial x)$.

If there are only minimal changes in intake flow properties in the time it takes a slice of gas to pass through the scramjet duct (one flow length), the flow can be analyzed using a steady flow analysis using the average intake flow properties. This quasi-steady approach can be justified when the errors introduced by ignoring the transient terms is much less than other unknowns and the measurement uncertainties. For the case of *weak* transient inflow, it is useful to normalize values along the duct using an inlet flow parameter, so that comparisons may be made to axial distributions of properties between varying times. This means that all pressure measurements can be related to the time when the same physical slice of gas was at pressure the transducer. Using the *hypersonic equivalence principle* with constant axial velocity, the normalized flow property, $\hat{\lambda}(x, t)$, is calculated using Eq. (2), in which the time delay Δt is given as the nominal transit time from the reference position [Eq. (3)]. Thus, each individual fluid parcel is normalized against its initial state. Therefore, to the first order, this removes most of the influence of the change in inflow conditions. This type of normalization has been labeled the *initial reference method* [18]:

$$\hat{\lambda}(x_n, t) = \frac{\lambda(x_n, t)}{\lambda(x_{\text{ref}}, t - \Delta t)} \quad (2)$$

$$\Delta t = \frac{(x_n - x_{\text{ref}})}{U_{\text{norm}}} \quad (3)$$

When changes in inflow properties are more significant along the length of the scramjet, further analysis is required. For these *stronger* transient changes in inflow, a *quasi-steady* analysis may be used, where the change in the local term of a flow property is insignificant compared with the convective term:

$$\frac{\partial\lambda}{\partial t} \ll U \frac{\partial\lambda}{\partial x}$$

This is where data can be compared to a steady flow analysis by gathering the flow data for the same slice of gas at all relevant axial locations as it travels through the scramjet (i.e., the time of entrance t , plus an offset time Δt). If a quasi-steady analysis can be applied, transient inflow can allow for multiple different inflow conditions to be tested during one test. Also, the normalization procedure will need to be altered for a quasi-steady analysis to Eq. (4). This normalization method has been labeled the *slug-tracking method*. Both of these methods normalize the gas slices at the measurement locations by their initial values at the normalization location. The difference being, the slug-tracking method presents the normalized data for a single slice of gas with a set of initial properties, rather than multiple gas slices that had different initial properties, which at a single point in time are at the measurement locations. If the freestream of the experiment being conducted is transient, analysis should be provided to verify the appropriateness of the normalization technique used:

$$\hat{\lambda}(x_n, t) = \frac{\lambda(x_n, t + \Delta t)}{\lambda(x_{\text{ref}}, t)} \quad (4)$$

Previous calculations of scramjet combustors with transient inflows, which reflect those produced in reflected shock tunnels, have been undertaken by Jacobs et al. [19] and Rogers and Weidner [20]. However, the results from these simulations were used to determine the time required until flow establishment had been achieved by a linear change in flow properties. Because static pressure is the only flow property to be measured experimentally, the nature of this flow property is of most importance for this current study. In scramjets, large pressure changes will occur through the intake, combustor and

thrust nozzle. Therefore, substantial convective terms are expected throughout the entire engine. To determine if a quasi-steady analysis can be used to analyze both the experimental and calculated static pressures, local and convective terms in the *total derivative* are compared with the computational simulations of the intake (without fueling), using the transient inflow properties previously described. These simulation data are then used to evaluate the two *quasi-steady* normalization methods.

A. Transient Numerical Calculation

To provide both a means of determining the nature of the pressure measurements and also a qualitative check of the flow processes within the scramjet, a time-dependent numerical calculation of the airflow through the experimental scramjet engine is presented. With this simulation reflecting the true startup flow that will pass through the inlet of the engine, the *impulsive starting* of the scramjet intake [21] in an expansion tube can also be investigated. Since the main purpose of this calculation is to study the effects of transients on the measurements, several assumptions are made to simplify the calculation to make it possible with the available computing power (limited to one week using 58 computer processors). These assumptions are as follows:

- 1) Simulation is for a fuel-off experiment.
- 2) Blunt leading edges are ignored.
- 3) A grid-resolved boundary layer may not be achieved, especially during flow startup when it is growing from zero thickness.

The gas model used for the calculation assumed a state of both thermal and chemical equilibrium for the air. The geometry for the simulation can be seen in Fig. 4, which also shows a representation of the grid. The number of cells located axially in the simulation is 1540, with 100 cells spanning the transverse direction across the combustor. Clustering of the grid was applied in the transverse direction toward the body and the cowl sidewalls, to increase the number of cells in the boundary layer. Inflow is from the left boundary, with outflow through both the right and bottom boundaries of the inlet and the far right boundary. The simulation used the Baldwin-Lomax turbulence model, which was applied to all body-side surfaces except for the first wedge where the boundary layer assumed to be laminar. The cowl wall boundary layer was simulated to be laminar, but in the physical testing, the boundary layer will transition a short distance from the leading edge. As turbulent boundary layers develop faster than laminar, this is a conservative approach for defining the limits of steady flow. All walls are assumed to be at a fixed temperature of 300 K.

The inflow for the scramjet calculation needs to reflect that produced in the actual facility. To achieve this, previous calculations [11] using a hybrid method of numerical simulation of the expansion-tube flow processes were used to provide the transient history of inflow properties to the scramjet entrance. Radial and axial variations produced by the facility in the region of the scramjet intake are minimal ($\pm 2\%$) and were not included. The transient history of flow properties used as inflow into the scramjet (i.e., freestream conditions) can be seen in Fig. 5, which were taken at 10 mm from the centerline of the nozzle exit. This shows that the static pressure is the

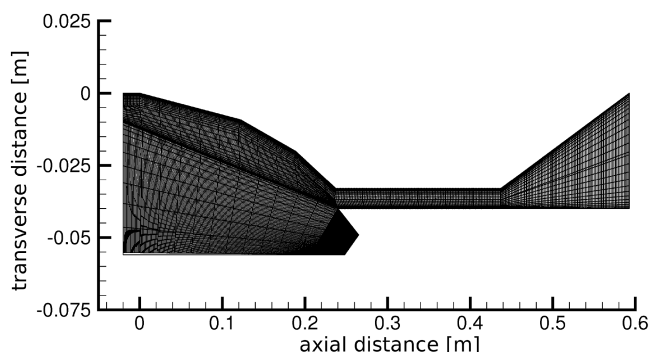


Fig. 4 Simulation domain for transient scramjet simulation. Every sixth line is shown in the mesh for each block.

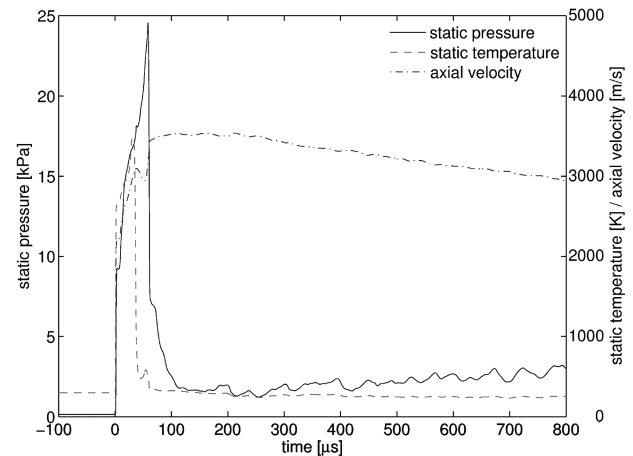


Fig. 5 Inflow properties for transient simulation of scramjet geometry using the effective freestream of the expansion tunnel. Properties are taken at 16 mm from centerline at nozzle exit from numerical simulation of X2 Mach 10 flow condition [11].

last property to stabilize after the nozzle startup period, with all properties deviating at approximately $220 \mu\text{s}$.

As a check on grid resolution, a second calculation that used two-thirds of the number of cells found that the maximum difference in wall pressure throughout the engine was 5% [11]. As this maximum difference was caused locally due to the small changes in the axial location of the cowl return shock, and differences of less than 1% were recorded elsewhere, this simulation was deemed to have enough resolution to capture the transient effects to undertake this study.

B. Results of Simulation

The transient numerical simulation of the scramjet experiment showed that quasi-steady supersonic flow was established within the duct. The flow passes through a series of shocks and expansions within the constant area combustor and is then expanded out through the nozzle without any choking or unstart effects. To provide an overview of the flow, Fig. 6 shows static pressure contours in the scramjet at $500 \mu\text{s}$. The intake shows three shocks being produced that pass just outside the cowl edge. The combustor flow is fairly nonuniform; shock and expansion waves cross the combustor, and a large separation region exists where the cowl shock impinges the body-side boundary layer. This separation region would be undesirable in an operating scramjet [21]; however, it is not an issue for this testbed scramjet unless it grows large enough to unstart the intake. The shocks in the combustor are seen to become weaker by the end of the combustor. No major waves can be seen on the thrust surface, since as the flow reaches the combustor exit, most of the strong waves have been dispersed out and there are generally low pressures in this region.

Path lines[§] are overlaid onto the contour, indicating the paths of different fluid particles as they would travel through the engine, ignoring the transient effects. The bulk of the flow through the combustor is at an average pressure of 60 kPa and temperature of 1000 K, which is sufficient for ignition of hydrogen. However, at the start of the combustor on the cowl side (where the bulk of the flow passes), the air gets compressed to 200 kPa and 1200 K, which will dramatically decrease the ignition time. The axial flow speed does not change significantly through the entire engine (decreasing by 200 m/s); therefore, the assumption of a constant velocity in the normalization procedure shown above is appropriate. The average flow Mach number seen through the combustor is 4.8.

By studying the static pressure along the wall side at single instants in time (Fig. 7), the scramjet flow can be seen to be dominated by a series of discrete waves. The inlet flow has three distinct pressure

[§]Path lines mark the flow particles path through the velocity contour field, ignoring that the field will be changing in time.

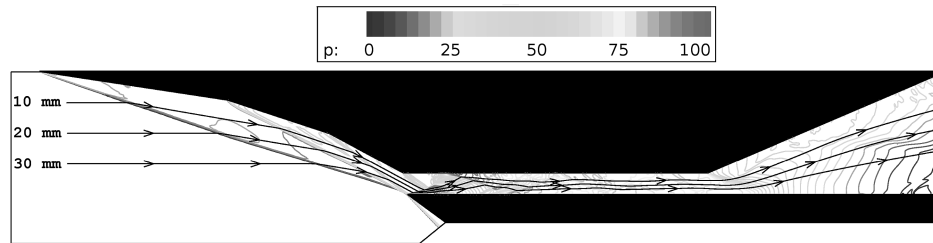


Fig. 6 Static pressure and path lines within scramjet from transient simulation at 500 μ s. Diagram is scaled by a factor of 2 in the transverse direction. Units are in kilopascals.

levels, for each of the three shock waves generated by the wedges. The pressure then drops as the flow expands around the corner into the combustor to align with the freestream, then increases dramatically as the cowl shock impinges the body-side boundary layer, separating it. A series of shock and expansion waves are then present along the length of the constant area combustor. Finally, the flow is then rapidly expanded around the aft corner of the combustor onto the thrust surface, where the largest force is applied just after the combustor. The flow structure is seen to be qualitatively similar at each of the three times presented, but the values are offset by differences caused by the inflow properties. This indicates that if quasi-steady flow assumption is valid, a normalization procedure may be applicable to analyze data at various times. Interestingly, the pressure on the thrust surface is similar for all three cases, indicating a higher drag at later times with the pressure on the inlet increasing with time.

The intake region was chosen for evaluation, as it represents a critical part of the engine that exhibits changes due to both the local transient and convective terms. As the flow through the scramjet intake of this study is dominated by discrete shock waves, the change in the convective terms will be large at the shock locations and small in between. Therefore, evaluation of the convective terms is undertaken along a path line at a given time (in a laboratory reference, which assumes steady flow velocity), using the initial position, velocity and pressure as a reference. The local term is then evaluated for path lines originating at the same position, but at two different times (Fig. 8). The path line used originates in the middle of the capture area of the freestream, which then passes through the series of oblique shocks on the intake (Fig. 6). The change in location of the actual streamline over the time taken to evaluate the local terms is shown to be negligible by comparing the paths of the two path lines. However, the change in pressure over this time is significant, with a rise of 25% (Fig. 8a). The comparison of the axial convective terms and the local terms along the path line are shown in Fig. 8b. The convective terms throughout the intake are seen to be two orders of

magnitude larger than the local time derivative terms and hardly change between 500 and 600 μ s. The change in the convective term across the intake is 0.67 kPa/ μ s, compared to the temporal change in the combustor entrance of 0.012 kPa/ μ s. Also, each increase in the convective term across each shock is at least an order of magnitude larger than the local term. This shows that the convective terms are much larger than the local terms along the intake, and quasi-steady analysis should therefore be applicable.

A normalization procedure can be used to remove some of the long-time-duration effects caused by the transient inflow rise in static pressure, allowing a more accurate presentation of the data. Figure 9 shows a comparison of the normalization of pressure for the two methods along the body sidewall of the scramjet against simple normalization of the scramjet data (data are taken at one time and normalized using the current intake pressure). A slug of 10 μ s period was used, at a normalization velocity of 3100 m/s. Both methods of normalizing the pressure data show similar trends in the reflection and strength of the waves throughout the scramjet and reproduce the trends seen in the whole engine. Both methods are seen to perform quite well, with it being difficult to pick differences in the combustor of the engine. However, as there are noticeable differences between the three normalized data sets, it is concluded that the slug-tracking method is the most appropriate due to analyzing a gas slug of one initial set of flow properties. This is supported by the fact that the slug-tracking normalization method exhibits the lowest difference (less than 5% apart from shock locations).

The accuracy of these methods relies upon the accurate definition of the velocity of the gas through the scramjet. The velocity will not remain constant through the engine, as assumed in the normalization methods, which will cause inaccuracies in presented results. Also, the inflow velocity will change in time, calculated to be 12% over the test time (Fig. 5). The errors in these methods will increase for measurements taken further downstream from the normalization location, since the time differences will increase. To investigate this effect, a comparison is made between three constant normalization

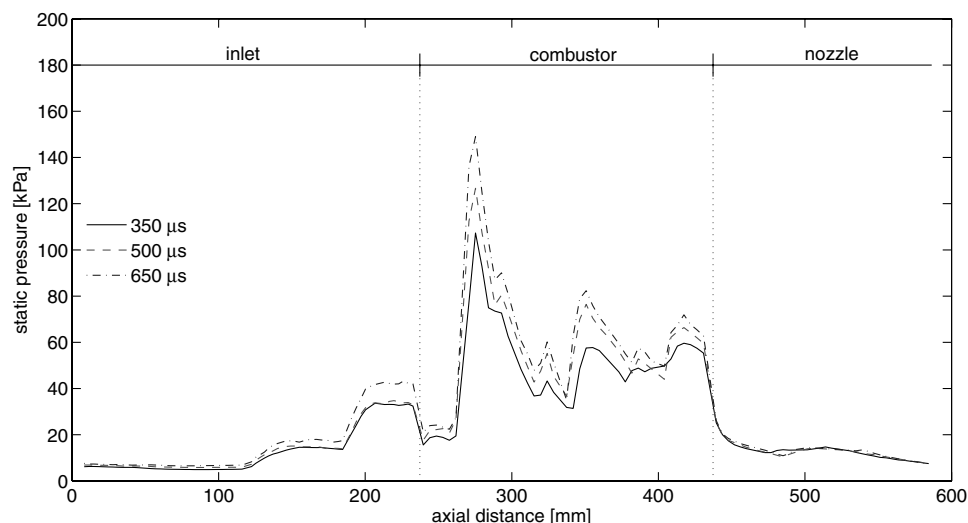
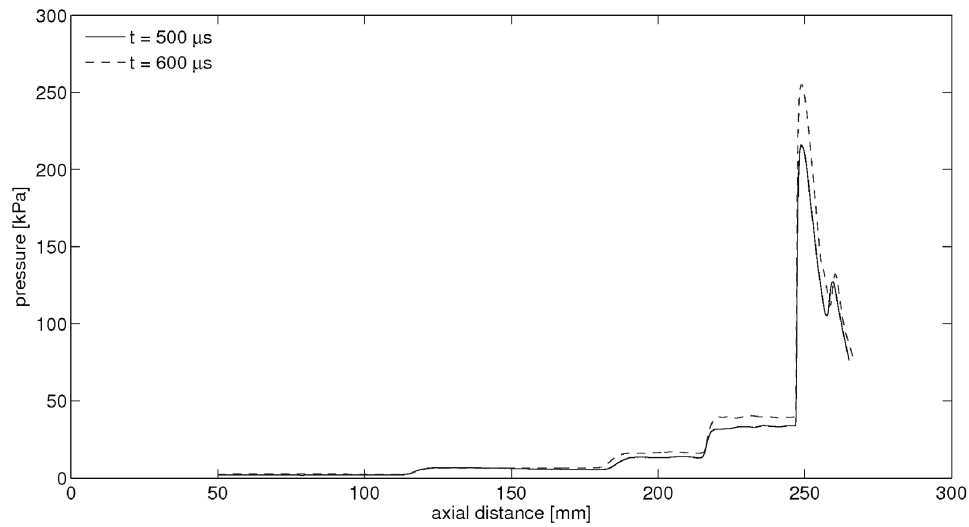
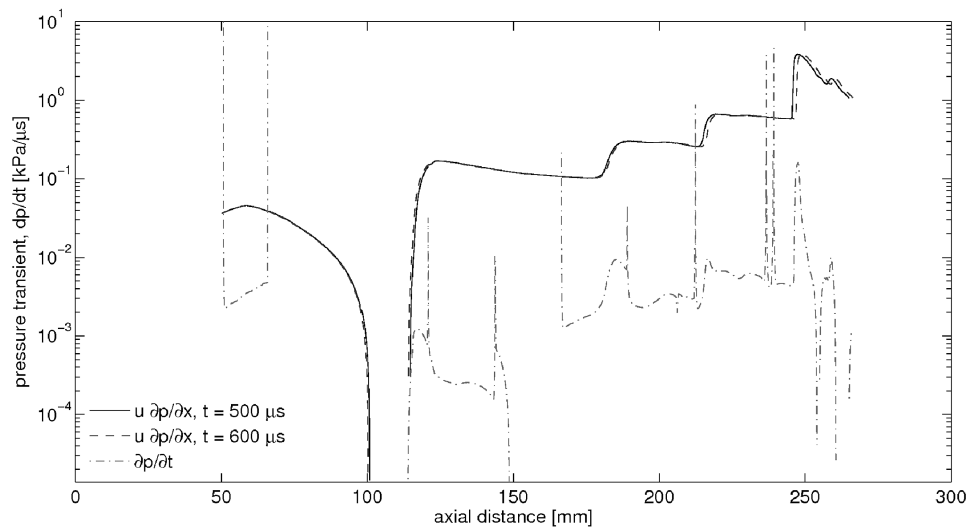


Fig. 7 Comparison of wall pressure along the body side of the scramjet duct from the numerical simulation at various times, averaged over a 10 μ s period.



a) Static pressure



b) Pressure derivative terms

Fig. 8 Evaluation of appropriateness of quasi-steady analysis by taking path lines through intake flow at 500 and 600 μs . Starting position for path line is $x = 50 \text{ mm}$ and $y = -20 \text{ mm}$.

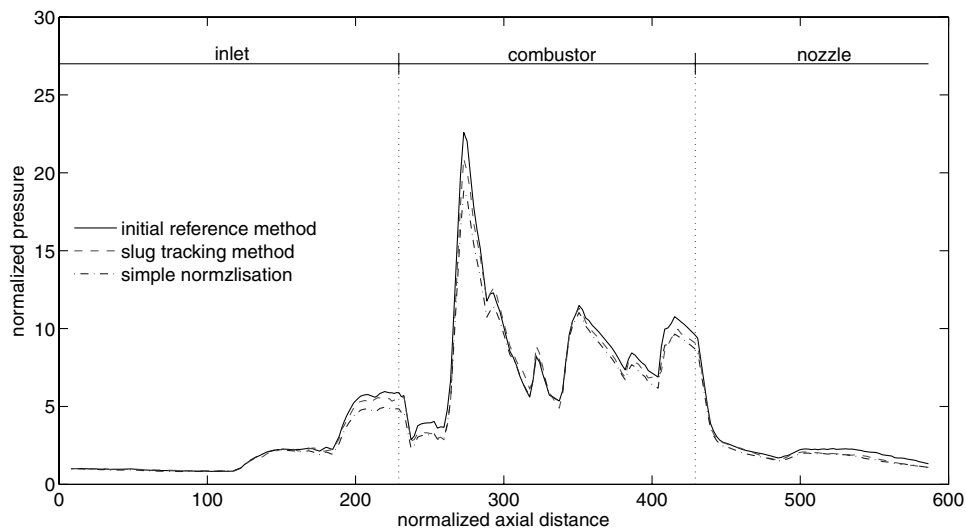


Fig. 9 Comparison of different normalization methods for transient data at 500 μs . Normalization velocity of 3100 m/s, averaged over a 10 μs period.

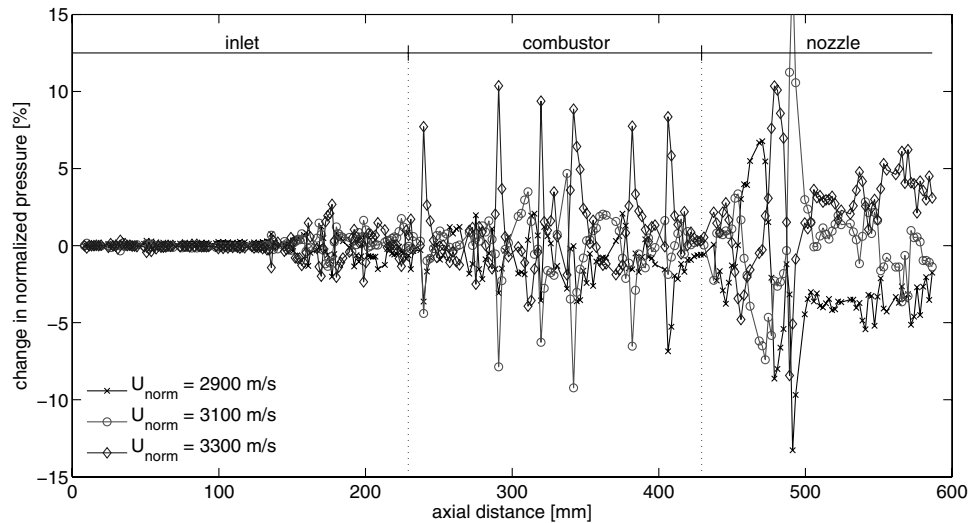


Fig. 10 Discrepancy in slug-tracking method caused by error in assuming a constant normalization velocity at $500 \mu\text{s}$.

velocities (which range over the axial velocities minimums and maximums through the engine in the test period) and a varying normalization velocity taken from a path line (Fig. 6) for the slug-tracking method in Fig. 10. As the path line is taken from the scramjet at one time (i.e., a snapshot is taken of the flow, as if the engine was in steady state at that time), the time that this is taken from the solution is approximately half of the time of flight of a particle through the engine. The difference between the time delay [Eq. (3)] through the engine shows that the variation for 3100 m/s is quite small (less than $5 \mu\text{s}$ throughout the engine). Also, both of the other normalization velocities show relatively small time delay differences, which by the end of the duct becoming less $15 \mu\text{s}$. The comparison between the normalized pressure that uses the varying normalization velocity to the constant 3100 m/s, shows there are only minor differences (Fig. 10). Along the intake this difference is less than 1% and only increases to 4% by the thrust surface (ignoring the large spikes due to movement in waves). The small movement of waves does not change the average pressure significantly, although the location of the peaks may give an apparently large local error as a given shock wave traverses the plotted axial location. Thus, the time of flight through the engine is quite small and the errors associated with the constant normalization velocities are also small.

Applying this method to a scramjet engine experiment in which there is a transient freestream, can allow the experimenter to provide quasi-steady estimates of pressure field through the engine. This method of analysis could be limited when the effects of fuel injection

and combustion are considered. The fuel injection process is separate to that of the freestream flow generation and is steady over a much longer period. For some flow conditions, the freestream properties change more rapidly than those of the injected fuel stream. In these situations the flow equivalence ratio will be changing with time, but the relevant steady flow conditions can still be reproduced by the analysis presented, provided the quasi-steady flow conditions apply. If the transient terms in the conservation equations are very much less than the convective terms, then the quasi steady analysis will also still apply in a combustoring situation. However, supersonic combustion in constant area ducts is associated with significant decreases in velocity. This can be overcome with a description of the velocity change throughout the engine as to ensure that the same slice of gas is analyzed. The coupling of the chemical reaction rates to the incoming flow properties will be harder to deal with and in the absence of time accurate computational simulations of the engine (due to the prohibitively large computational expense), which include the temporal inflow, fuel injection and combustion, this method will at least give a first-order representation of the flow.

IV. Experimental Results

The scramjet test program involved varying the parameters of test gas (air or nitrogen) and fuel equivalence ratio. Results are analyzed using the slug tracing method described previously, in order to correctly couple the data with the transient freestream condition. All

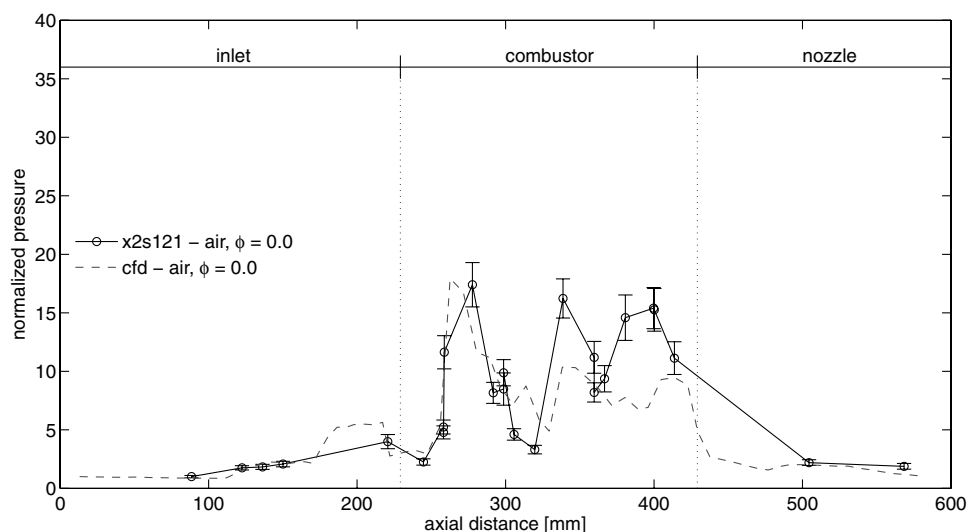
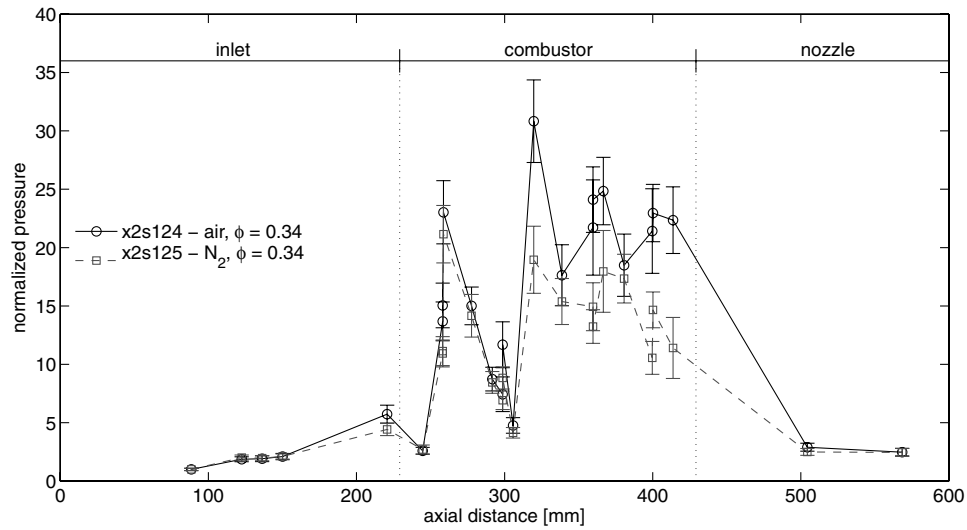
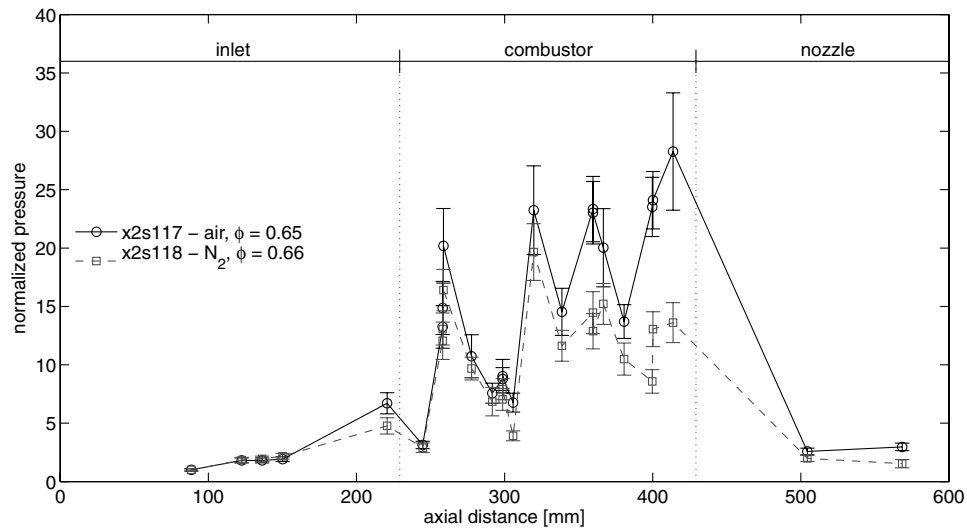


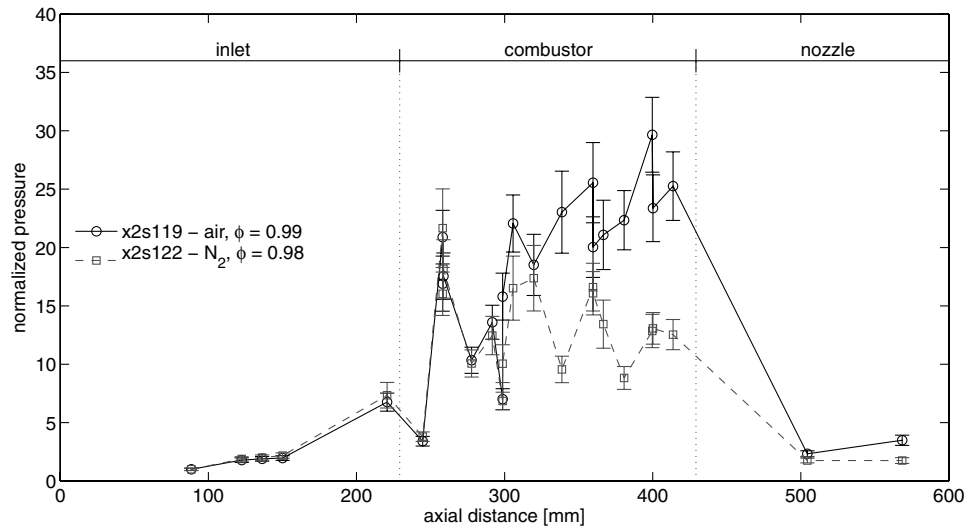
Fig. 11 Comparison of experimental with computational simulations with fuel off. Plotted using slug-tracking method at $500 \mu\text{s}$.



a) Low equivalence ratio



b) Medium equivalence ratio



c) High equivalence ratio

Fig. 12 Effects of combustion on body-side static pressure measurements along the scramjet for various mass fuel rates. Plotted using the slug-tracking method at 500 μ s.

plots showing the axial distributions at a given time are averaged results over $10\ \mu\text{s}$ (or slug lengths of approximately 30 mm), to mitigate the effect of shifts in the wave structure within the scramjet. Lines between data points are given for visual clarity and do not indicate linear trends between data points. The normalization pressure for each shot and time is taken from the first pressure transducer on the intake. A constant normalization velocity of 3100 m/s is used for all shots. This corresponds to the average velocity through the scramjet as calculated numerically and for fuel-off shots is shown to be the most accurate (Fig. 10). Also, the mass flow rate of air into the combustor at $500\ \mu\text{s}$ is $0.1586\ \text{kg/m}^3$, taking the mass capture ratio from the numerical simulation of 0.92. All pressure traces used are referenced against the preshock values to remove any offset in the traces. Individual time histories of wall pressures are presented and reviewed in McGilvray et al. [13].

Scramjets have inherent unsteadiness in the flow due to turbulent boundary layers, combustion processes and variations caused by movement of shock trains from this turbulence [22]. However, it is convenient to present scramjet point measurements as averaged values, which will have an associated uncertainty due to sampling an unsteady signal and uncertainty from the measurement technique. Further complexity is added in this experiment by the transient freestream (both freestream noise and bulk transient behavior), causing unpredictable uncertainties in both space and time dimensions. Modeling of the transient nature of the inflow and prediction of measurement uncertainties in the duct is needed to define the experimental uncertainty levels [11]. This accounts for uncertainties in the pressure transducer measurements, uncertainty in sampling the mean over a finite period and uncertainty due using a constant normalization velocity. Shot-to-shot variation is a different issue. For any specific shot, the uncertainties can be calculated, apart from the effect of differences in fuel equivalence ratio throughout the engine.

A direct comparison is made between the transient numerical simulation and fuel-off scramjet data (Fig. 11), to check the methodology established from the calculations is reflected in the experimental results. Throughout the scramjet, the numerical simulation is similar in behavior to the experimental measurements. The mean level of pressure in the combustor agrees well between the two sets of data. However, the shock/expansion locations are slightly different. This is to be expected, since the blunt leading edges were not included in the simulation. The computational simulation exhibits a weaker wave structure toward the end of the combustor (Fig. 6) and a higher average pressure in the second half of the combustor. The pressures measured on the thrust surface agree well with the computational simulation results, noting there are weaker waves in the numerical simulation at the combustor exit. As the

calculation neglects the effects of the sidewalls being two-dimensional, and assuming a laminar cowl wall boundary layer, the experimental flow structure is well represented by the numerical simulation.

Combustion effects were investigated by a comparison of normalized static pressure distributions along the scramjet, between shots with a nitrogen test gas (*tare* shots) and shots with an air test gas (*combustion* shots) for similar fuel mass flow rates. The only significant change between the two tests should be due to the combustion of the fuel. For supersonic combustion in a constant area duct, the static pressure should, on average, increase along the combustion chamber. Figure 12 presents data for the same inflow properties at $500\ \mu\text{s}$, but for three fuel equivalence ratios ($\phi = 0.33, 0.65, \text{ and } 0.99$). The change in fuel equivalence ratio was achieved by varying the fuel mass flow rate. All three fuel equivalence ratio cases exhibit the same pressure profiles within the uncertainty bands between the combustion and tare cases up to 300 mm. After this point, substantial reaction of the hydrogen air mixture is indicated by a large increase in the pressure in the air case that was not present in the tare case. The large increase in mass fuel flow rate does not have a significant effect on the pressure change by the end of the combustor or on the thrust surface. The pressure rise from combustion across the combustor for a premixed hydrogen/air flow (assuming perfect gas and no losses) in a constant area duct is calculated for a heat release of $90\ \text{MJ/kg}$ at the tested fuel equivalence ratios. Comparing this to the experimental pressure rise indicates that full heat release has not occurred in any of the experiments. With the experimental pressure rise across the combustor at lower equivalence ratios being closer to the premixed calculation using the equivalent heat release, this indicates the flow is most likely mixing limited.

By considering different times during the experiment, the axial distribution of pressure will change due to differences in inflow properties (Fig. 13). The transient freestream will also alter the intake shock structure, fuel equivalence ratio, fuel penetration, and mixing, and therefore the combustion processes. From the normalized wall pressure measurements, the major effect seen is a slight shift in the shock structure in the combustor. However, the pressure levels do not vary greatly down the combustor. As the flow is dominated by discrete waves, further conclusions about the changes incurred due to changing inflow properties are limited by the lack of spatial resolution in the measurements.

The change in fuel equivalence ratio in these experiments occurred by altering the fuel mass flow rate each shot and also due to the change in inflow mass flow rate of air within a given shot. The effects of this variation in fuel equivalence ratio by these two causes is investigated in Fig. 14 by taking the normalized pressure at the exit (i.e., the last pressure transducer on the thrust surface). However, due

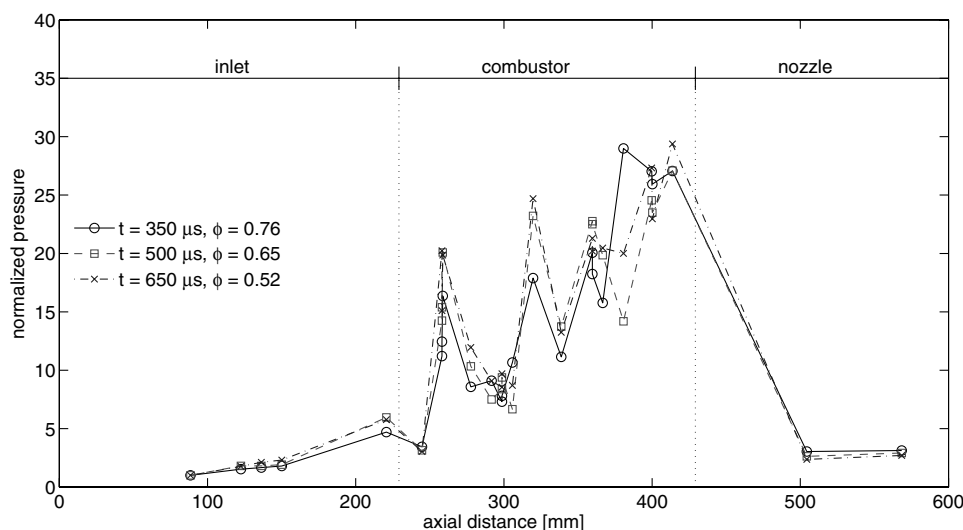


Fig. 13 Effect of variation of freestream on body-side static pressure measurements along the scramjet for combustion test. Plotted using slug-tracking method at $500\ \mu\text{s}$. Data are taken from shot x2s117. Error bars are not shown, for purposes of clarity.

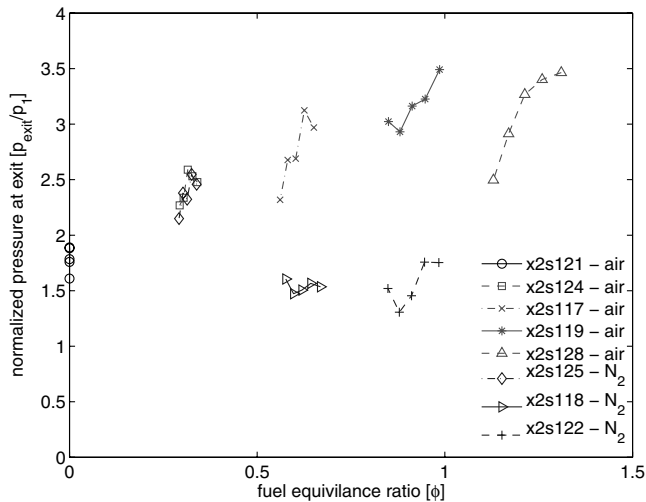


Fig. 14 Normalized exit pressure as a function of fuel equivalence ratio for Nitrogen or air freestreams. Plotted using slug-tracking method at 500, 550, 600, 650, and 700 μ s.

to the two-dimensional nature of the expansion process, this does not necessarily give an indication of the level of combustion achieved. As the pressure distribution developed along the thrust surface is dependent on the Mach number profile across the combustor's height, the pressure at a single point may be lower although the integrated inviscid thrust could be higher [23]. Also, it must be noted that the assumption of a constant velocity of gas slugs moving through the engine will have the greatest error when normalizing thrust surface data, especially in the presence of combustion, which will slow the flow in the constant area combustor. The results indicate that the difference between tare and combustion shots is quite noticeable at the higher equivalence ratios, with a higher normalized exit pressure. Fuel injection also has a net reduction in pressure from the no injection case (x2s121). However, at the lower equivalence ratio, the change in freestream gas exhibits little difference in the normalized pressure. This shows the difference in the combustor pressure measurements (Fig. 12a) has not resulted in a higher pressure at this location on the thrust surface. The change in fuel equivalence ratio caused by the increasing the air mass flow rate (changing inflow properties) is seen to sharply increase the normalized exit pressure, whereas a slower increase is seen by altering the fuel mass flow rate.

V. Conclusions

This study has shown a complete *nose-to-tail* test of a hydrogen-fueled scramjet can be successfully undertaken in an expansion-tunnel facility. The experiment was conducted at the total pressure limit of reflected shock tunnels capability to create scramjet conditions, a transition can now be made to using expansion tubes for testing the upper flight envelope of full engine geometry scramjets. The appropriateness of considering the flow as being in a quasi-steady state was investigated by the use of transient numerical simulations of the engine, where the inflow conditions reflected the time history of freestream flow properties. This analysis indicated that convection was the major driver for determining the pressure at a given axial location, rather than the local time derivative. A technique for analyzing quasi-steady scramjet point measurements throughout the engine was developed and applied to the numerical simulation. This method presents pressure data from different axial locations in the engine for a finite slug of gas, normalized against its initial state. Applying the normalization technique to the experimental data, both different fuel equivalence ratios and variation in inflow properties were analyzed. Also, by analyzing the data in this way, for a single experiment, measurements could be collected for various fuel equivalence ratios and inflow properties.

Based on this work, it is recommended that all scramjet or ducted flow experiments that are tested with transient inflows, especially

those undertaken in impulse facilities, should apply the slug-tracking method. This will remove shot-to-shot and bulk effects of the transient inflow variations in the data and will ensure accurate interpretation of the flow data. Further to this, evaluation of the transient analysis method may also be required for each new experiment/flow condition to ensure that errors introduced by ignoring local transient terms are negligible compared to other experimental uncertainties.

Acknowledgments

The authors would like to acknowledge the financial support of the Australian Research Council for the experiments. Financial support for the cluster computer was provided by SUN Microsystems and by the Queensland State government under the Smart State program. Also, the authors thank Brian Loughrey for his work in both model fabrication and facility maintenance. All the simulations detailed in this paper were undertaken on the Blackhole cluster computer located at the Centre for Hypersonics, University of Queensland. We thank Rainer Kirchhartz and Wilson Chan for running the University of Queensland Hypersonics cluster computer. Thanks to David Gildfind for providing critical input to the paper.

References

- [1] Billig, F., "Research on Supersonic Combustion," *Journal of Propulsion and Power*, Vol. 9, No. 4, July–Aug. 1993, pp. 499–514. doi:10.2514/3.23652
- [2] Chinitz, W., Erdos, J. I., Rizkalla, O., Anderson, G. Y., and Bushnell, D. M., "Facility Opportunities and Associated Stream Chemistry Considerations for Hypersonic Air-Breathing Propulsion," *Journal of Propulsion and Power*, Vol. 10, No. 1, 1994, pp. 6–17. doi:10.2514/3.23705
- [3] Curran, E. T., "Scramjet Engines: The First Forty Years," *Journal of Propulsion and Power*, Vol. 17, No. 6, Nov.–Dec. 2001, pp. 1138–1148. doi:10.2514/2.5875
- [4] Rizkalla, O., Bakos, R., M. V., P., Chinitz, W., and Erdos, J., "Use of an Expansion Tube to Examine Scramjet Combustion at Hypersonic Velocities," AIAA/ASME/SAE/ASEE 25th Joint Propulsion Conference, AIAA Paper 89-2536, June 1989.
- [5] Erdos, J., and Bakos, R., "Prospects for a Quiet Hypervelocity Shock-Expansion Tunnel," 18th AIAA Aerospace Ground Testing Conference, AIAA Paper 94-2500, June 1994.
- [6] Erdos, J., Calleja, J., and Tamango, J., "Increase in the Hypervelocity Test Envelope of the HYPULSE Shock-Expansion Tube," AIAA Paper 94-2524, June 1994.
- [7] Bakos, R., Calleja, J., and Erdos, J., "An Experimental and Computational Study Leading to New Test Capabilities for the HYPULSE Facility with a Detonation Driver," 19th AIAA Advanced Measurement and Ground Testing Conference, AIAA Paper 96-2193, June 1996.
- [8] Erdos, J., Bakos, R., and Castrogiovanni, A., "Dual Mode Shock Expansion/Reflected Shock Tunnel," AIAA 35th Aerospace Sciences Meeting, AIAA Paper 97-0560, Jan. 1997.
- [9] Chue, R., Bakos, R., Tsai, C., and Betti, A., "Design of an Expansion Tunnel Nozzle in HYPULSE," *Shock Waves*, Vol. 13, 2003, pp. 261–270. doi:10.1007/s00193-003-0215-0
- [10] Tsai, C., and Bakos, R., "Mach 7-21 Flight Simulation in the HYPULSE Shock Tunnel," 23rd International Symposium on Shock Waves, Fort Worth, TX, July 2001.
- [11] McGilvray, M., "Scramjet Testing at High Enthalpies in Expansion Tube Facilities," Ph.D. Thesis, Univ. of Queensland, St. Lucia, Australia, 2008.
- [12] Scott, M., "Development and Modelling of Expansion Tubes," Ph.D. Thesis, Univ. of Queensland, St. Lucia, Australia, 2006.
- [13] McGilvray, M., Kirchhartz, R., and Jazra, T., "Comparison of Mach 10 Scramjet Measurements from Different Impulse Facilities," *AIAA Journal*, Vol. 48, No. 8, 2010, pp. 1647–1651. doi:10.2514/1.J050025
- [14] Pulsonetti, M. V., "Scaling Laws for Scramjets," Ph.D. Thesis, Univ. of Queensland, St. Lucia, Australia, 1995.
- [15] Hayne, M., "Hypervelocity Flow over Rearward Facing Steps," Ph.D. Thesis, Univ. of Queensland, St. Lucia, Australia, 2004.
- [16] Gardiner, A., Paull, A., and McIntyre, T., "Upstream Porthole Injection in a 2D Scramjet Model," *Shock Waves*, Vol. 11, 2002, pp. 369–375. doi:10.1007/s001930200120

- [17] White, F., *Fluid Mechanics*, McGraw-Hill, Boston, 4th ed., 1999.
- [18] Anderson, J., *Hypersonic and High Temperature Gas Dynamics*, McGraw-Hill, New York, 1989.
- [19] Jacobs, P., Rogers, R., Weidner, E., and Bittner, R., "Flow Establishment in a Generic Scramjet Combustor," *Journal of Propulsion and Power*, Vol. 8, No. 4, 1992, pp. 890–899.
doi:10.2514/3.23566
- [20] Rogers, R., and Weidner, E., "Scramjet Fuel-Air Mixing Establishment in a Pulse Facility," *Journal of Propulsion and Power*, Vol. 9, No. 1, Jan.–Feb. 1993, pp. 127–133.
doi:10.2514/3.11494
- [21] Van Wie, D., "Scramjet Inlets," *Scramjet Propulsion*, Vol. 189, Progress in Astronautics and Aeronautics, AIAA., Reston, VA, 2000, Chap. 7, pp. 447–511.
- [22] Anderson, G., Kumar, A., and Erdos, J., "Progress in Hypersonic Combustion Technology with Computation and Experiment," 2nd AIAA International Aerospace Planes Conference, AIAA Paper 90-5254, 1990.
- [23] Stalker, R., "Thermodynamics and Wave Processes in High Mach Number Propulsive Ducts," 27th AIAA Aerospace Sciences Meeting, AIAA Paper 89-0261, Jan. 1989.

R. Lucht
Associate Editor